

Ammonia Sensors Based on Composites of Carbon Nanotubes and Titanium Dioxide

Marciano Sánchez and Marina Rincón

*Centro de Investigación en Energía, Universidad Nacional Autónoma de México
México*

1. Introduction

Design of composite materials for ammonia (NH_3) sensing is important because of two main reasons: (1) NH_3 is the most common substitute for chlorofluorocarbons (CFCs) in cooling systems, and (2) most sensors show long recovery times at room temperature due to the tendency of ammonia to strongly interact with many substrates. Multiwalled carbon nanotubes (MWCNTs) have been used to sense polar molecules like carbon monoxide (CO), carbon dioxide (CO_2), NH_3 , water (H_2O), and ethanol ($\text{C}_2\text{H}_5\text{OH}$) (Ong et al., 2002; Valentini et al., 2004; Varghese et al., 2001), as well as non polar gases like helium (He) and nitrogen (N_2) (Adu et al., 2001). For carbon nanotubes, studies have shown that O_2 molecules are electron acceptors with substantial adsorption energies and charge transference, while NH_3 , N_2 , CO_2 , methane (CH_4), H_2O , hydrogen (H_2) and argon (Ar) are electron donors (Zhao et al., 2002). Adsorption in CNTs is determined by adsorption energy and availability of sites, with typically four different adsorption sites: external surface, grooves between CNTs on the bundle outside, pores inside CNTs, and interstitial channel between adjacent tubes inside the bundle (Stan & Cole, 1998; Williams & Eklund, 2000). Additionally, theoretical studies carried out by Jhi et al. about the electronic and magnetic properties of oxidized CNTs indicated their high potential as gas sensors. These studies demonstrated that the sensing mechanism of as prepared CNTs is more related to oxygen doping than to intrinsic properties, and depends on the structural defects caused by the synthesis methods (Jhi et al., 2000).

With the aim of increasing the response of CNTs to certain gases, some studies about substitutional functionalization of CNTs have been reported (Peng & Cho, 2003). Although boron (B) and nitrogen (N) doping improve the response to gases like CO and H_2O , B_xC_y nanotubes show stronger chemisorption, in contrast with the substitutional functionalization with nitrogen (Villalpando-Paez et al., 2004). Oxidation of CNTs in acid solutions to graft oxygen functional groups [i.e., carboxyl (COOH), hydroxyl (OH), and carbonyl (CO)] on CNT walls have been widely used to diversify the sensing options. Another strategy has been the fabrication of compound materials based on CNTs and metallic oxides. Espinoza et al. reported the use of metallic oxides-CNT composites based on commercial tin (SnO_2) and tungsten (WO_3) oxide powders, as well as sol gel TiO_2 materials, in the sensing of NO_2 and CO at room temperature and 150°C . Their results indicated a better performance for CNT/ SnO_2 and CNT/ WO_3 than for CNT/ TiO_2 , for the titania composite the sensor response was barely sizable (Espinoza et al., 2007).

Throughout this chapter, we will present the synthesis and performance of compound materials based on MWCNT/TiO₂ tested as resistor and capacitor ammonia sensors. The design aims for low cost room temperature sensors with good reversibility and fast recovery times. For sensor fabrication, both materials were prepared separately (*ex-situ*) and deposited in a multilayer configuration. By means of spacial and spectroscopic resolution techniques we were able to correlate sensor fabrication with performance. We will demonstrate that the *ex situ* method combined with substantial chemical oxidation of pretreated CNTs provide the best composite material with synergistic properties for ammonia sensing. Variations of capacitance were as high as 150%, while changes in resistance were one order of magnitude lower.

2. Experimental

2.1 Film elaboration techniques

MWCNT functionalization

MWCNTs were obtained from Nanostructured & Amorphous Materials Inc. (90 wt.%, outer diameter < 10 nm, length: 5-15 μm, tangled). To introduce oxygenated functional groups, CNTs were refluxed at 100°C for 6 h in acid solutions of 0.5 M sulphuric acid (H₂SO₄) with variable concentrations of nitric acid (HNO₃). Functionalized CNTs were labelled according to the concentration of HNO₃ (2.5M, 7.5M, 12.5M) as CNT-2.5, CNT-7.5 and CNT-12.5, CNTs without treatment were labeled as CNT-WT, composites were labeled as CMP with the number of the HNO₃ concentration used for chemical treatment. CNT inks were prepared mixing 10 mg of CNTs with 40 μL of triton X-100 in 5 mL of deionized water, the triton/CNT weight ratio was 0.6.

Sensor fabrication (*ex-situ* method)

To prepare TiO₂ films, 100 mL sol gel baths containing 92 mL of isopropanol, 0.1 mL of hydrochloric acid (HCl), and 8 mL of titanium isopropoxide were kept at room temperature (27°C) for 24-48 h. Films were deposited by dip coating on glass (Corning) and indium tin oxide (ITO) 1x1.5 in substrates, using 8 dipping/withdrawing cycles at 30 mm/min speed, and air annealing for 5 min at 400°C after each immersion, and at 500°C for 1 h after the last cycle. After TiO₂ deposition, 0.5 mL of CNT ink was drop casted on top and was dried at room temperature for 24 h. The two layer film was annealed in air for 30 min at 400°C, finally another TiO₂ film (8 cycles) were deposited to make a sandwich like configuration; the whole system was annealed at 400°C in air for 1 h.

2.2 Characterization

The changes in chemical composition caused by the functionalization of CNTs were followed by thermogravimetric analysis (TGA, TA Instruments Q500). TGA studies were carried out under 5 mL/min oxygen flow and using 5°C/min heating rate in the 25-800°C temperature range. Particle size and zeta potential (ζ) were measured by dynamic light scattering (DLS, Zetasizer Nano, Malvern Instruments) as a function of CNTs functionalization. Film crystallinity was monitored by X-ray diffraction (Rigaku Dmax 2200, CuKα radiation, λ=1.5405 Å), using the Debye-Scherrer equation (Cullity, 1978) for crystallite size determination. Atomic force microscopy was used for surface microstructural studies (Nanosurf Easyscan, Nanosurf AG, Switzerland). The experimental setup for sensing trials for both platforms is shown in Figure 1, basically, nitrogen was passed through a bubbler

containing ammonia and was injected into a flask where the resistance or capacitance of the sensors changed as they were exposed to ammonia; the baseline was measured in dry air and the sensor in the picture correspond to a resistor sensor.

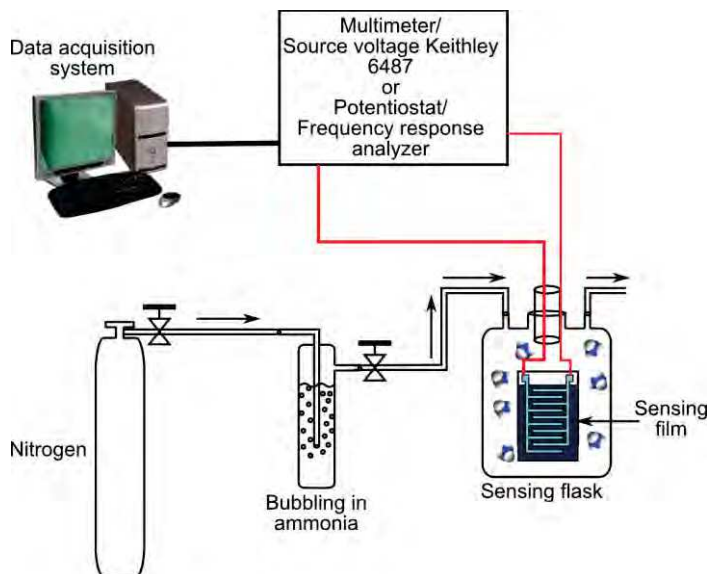


Fig. 1. Experimental setup used for sensing trials

For capacitor sensors, variations of capacitance were followed by electrochemical impedance spectroscopy (EIS) measurements in an Autolab PGSTAT302N potentiostat/galvanostat unit (Eco Chemie), using the configuration depicted in Figure 2. A perturbation of 5-10 mV was applied at open circuit potential in the frequency range from 10^5 to 10^{-3} Hz. Complex non linear least squares (CNLS) fitting of the experimental data was done with the Zsimpwin software (Princeton Applied Research). All the sensing trials were done at room temperature (27°C).

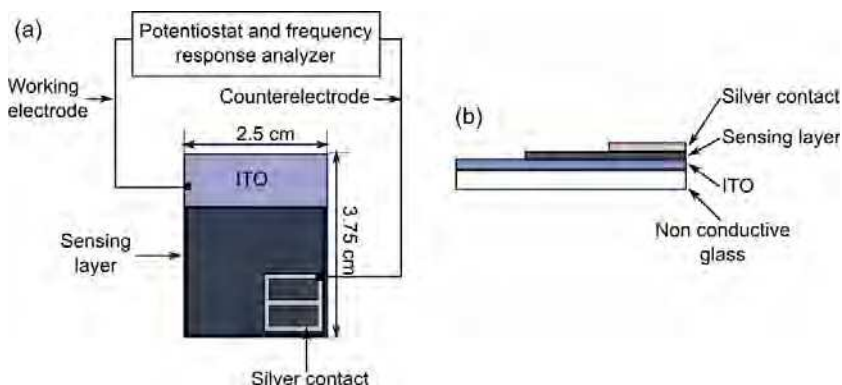


Fig. 2. Capacitor sensor configuration: (a) top view; (b) side view

3. Results and discussion

3.1 CNT characterization

Figure 3 shows the TGA curves of CNTs exposed to various acid treatments. From the variation of mass vs. temperature [Figure 3(a)], or mass/temperature ratio vs. temperature [Figure 3(b)] figures it is easy to appreciate the ~15 wt.% of metal and impurities content of as received CNTs (CNT-WT) as well as its removal by all the acid treatments. The higher oxidation temperature indicates that the treatment used for CNT-2.5 does not damage the nanotube surface, but as the aggressiveness of the functionalization increases, a sizable weakening of the CNT structures is observed, in addition to the grafting of oxygenated functional groups, as evidenced in Fourier transform infrared studies (Sánchez & Rincón, 2009). DLS characterization of CNT aqueous inks prepared with a triton/CNT ratio of 0.6 and sonicated for 30 and 90 min is presented in Figure 4. Ultrasonic treatments of 90 min produced a better dispersion, especially for CNT-WT and CNT-2.5, however, for CNT-7.5 and CNT-12.5 the differences between 30 and 90 min sonication times are smaller [Figure 4(a)]. The absolute value of ζ [Figure 4(b)] shows a continuous increase as the intensity of the chemical treatment does, up to ~18 mV, which is lower than the characteristic values of stable solutions (± 30 mV), this increase confirms the presence of functional groups, however in the long term these solutions would show a tendency to precipitate.

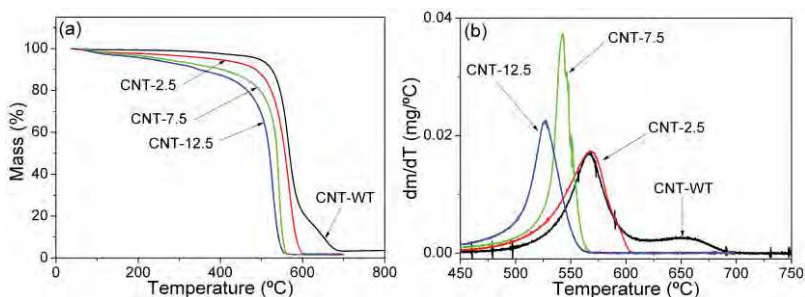


Fig. 3. Thermogravimetric analysis of CNTs in a 5 mL/min oxygen flow and heating ratio of 5°C/min: (a) mass vs. temperature; (b) mass/temperature ratio vs. temperature

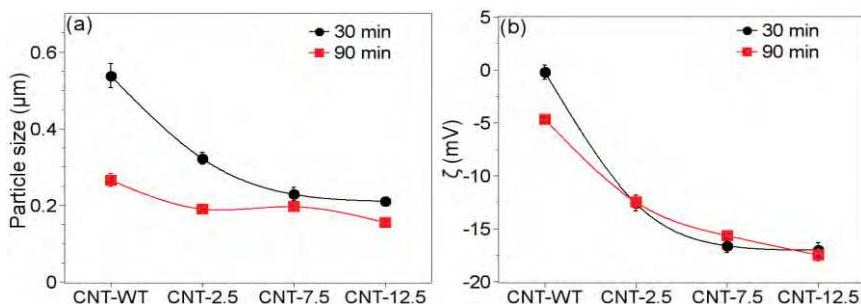


Fig. 4. Dynamic light scattering characterization of CNT inks based on sonication time and functionalization intensity: (a) particle size vs CNT functionalization; (b) ζ potential vs. CNT functionalization

3.2 Structural characterization

The effect of CNT functionalization on the topography of the composite is shown in Figure 5. Figures 5(a-b) show the surface and edge detection of CMP-WT composite. Several longitudinal and tangled formations of CNTs bundled in ropes are evident. In contrast, Figures 5(c-d) show images of CMP-12.5 composite, where CNT/titania grains are slightly smaller, more dispersed, and with shorter ropes. Analysis at a lower scale (not shown) confirmed that a compact and thin layer (~ 20 nm) of titania was formed covering all the surface including carbon nanotubes, with an increasing thickness as the intensity of chemical treatment does.

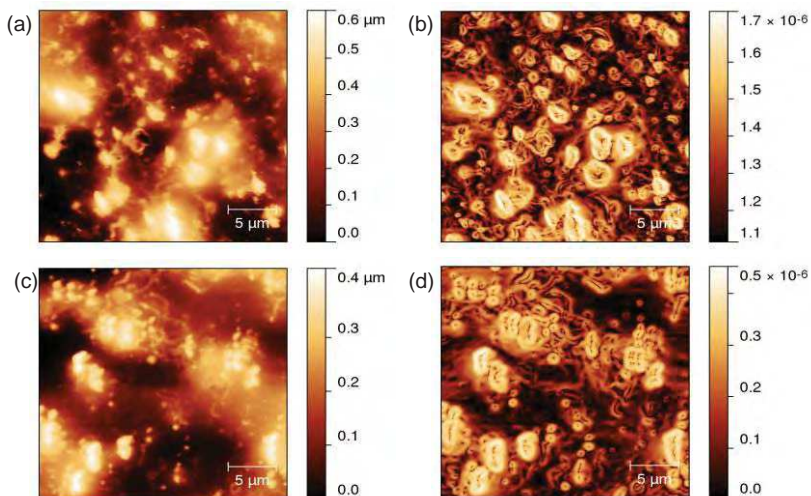


Fig. 5. AFM studies of $\text{TiO}_2/\text{CNT}/\text{TiO}_2$ composites deposited on glass substrates: (a) topography of CMP-WT; (b) edge detection on Fig. (a) showing CNT ropes; (c) topography of CMP-12.5; (d) edge detection on Fig. (c)

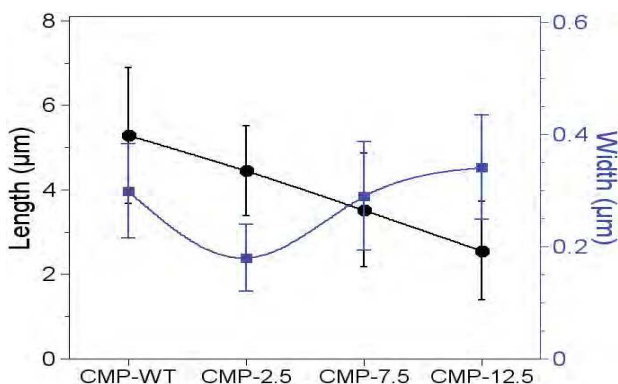


Fig. 6. Length and width of CNT ropes of $\text{TiO}_2/\text{CNT}/\text{TiO}_2$ composites deposited on glass substrates

Statistical analysis of the length and width of CNT ropes in TiO₂/CNT composites deposited on insulator glass substrates is shown in Figure 6. This graph confirms that the chemical treatment reduces the length of ropes from ~5 μm for CMP-WT to ~2.5 μm for CMP-12.5. A slight increase in the width is observed as the intensity of functionalization increases, which can only be due to a thicker titania layer, given that thinner CNT ropes are obtained at stronger functionalizations.

X-ray diffraction studies (Figure 7) of films prepared in a multilayer configuration (system TiO₂/CNT/TiO₂) shows only the anatase phase and broadening of its peaks. Crystallite size determination using the peak at $2\theta \approx 48^\circ$ (to avoid interference from carbon diffraction at $2\theta = 25^\circ$) shows a decrease from ~25 nm for CMP-WT to ~10 nm for CMP-12.5 (a reduction of ~60%), according to some studies that report the confined growing of titania grains attached to functionalized CNTs which are smaller than the ones growing away from nanotubes (An et al., 2007; Hieu et al., 2008; Song et al., 2007; Yu et al., 2007). This figure also confirms that CNTs with more functional groups are covered with a thicker titania layer.

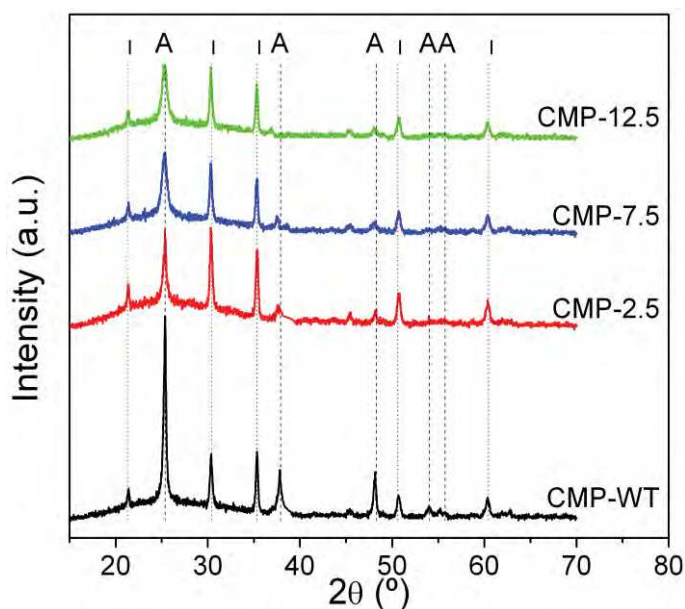


Fig. 7. X-ray diffraction patterns of multilayer systems TiO₂/CNT/TiO₂ deposited on ITO substrates. A: anatase; I: ITO.

3.3 Electrical characterization

3.3.1 Resistor sensors

In this section the performance of CNTs and TiO₂/CNT films as resistor ammonia sensors is presented. Figures 8-10 compare the effect of CNT functionalization on the dynamical response to 1 vol.% ammonia of CNT (Figure 8), CNT/TiO₂ (Figure 9), and TiO₂/CNT/TiO₂ (Fig. 10). Some of these figures show passivation of the most reactive sites during the first pulse, and reversible responses in the subsequent pulses.

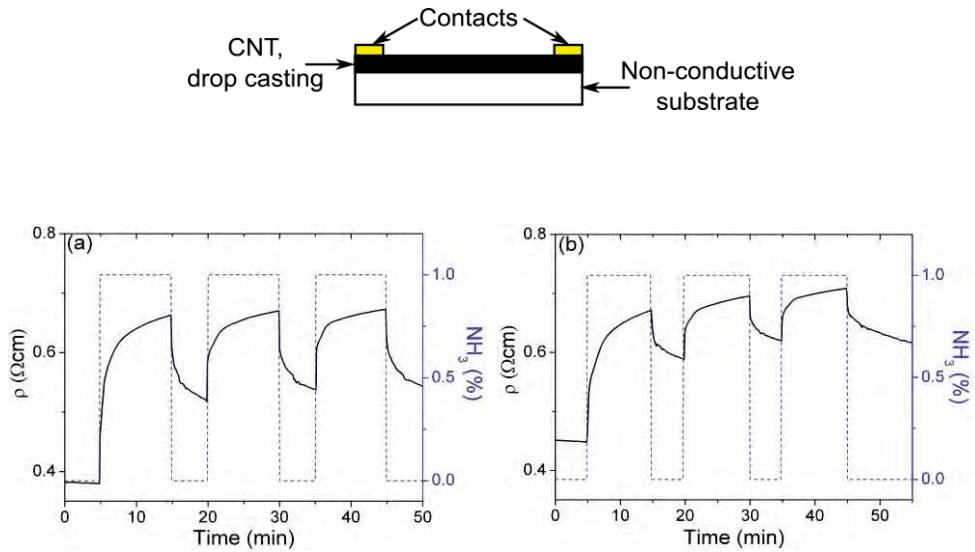


Fig. 8. Dynamical reponse to ammonia of CNT resistor films deposited by drop casting: (a) CNT-WT; (b) CNT-2.5

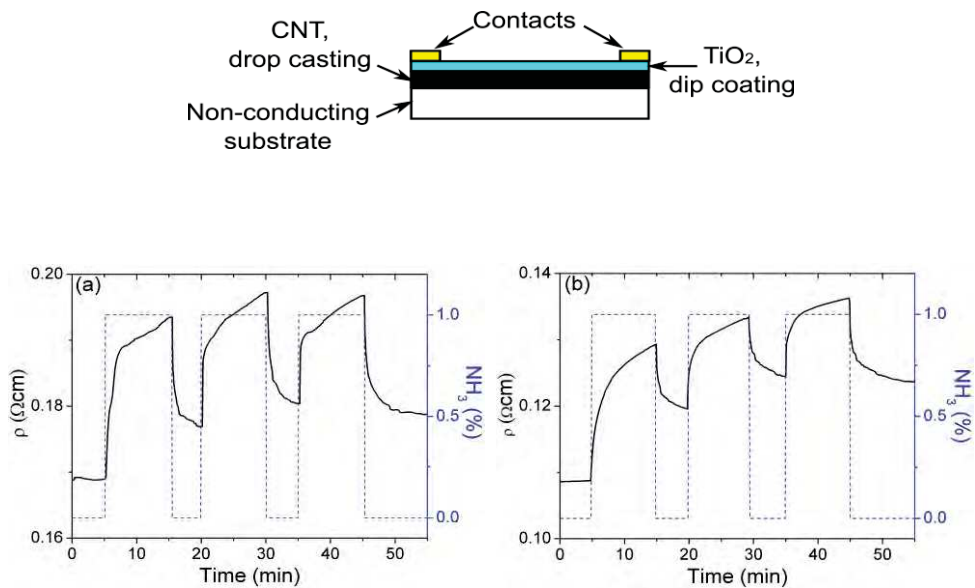


Fig. 9. Dynamical response to ammonia of compound films of CNTs (drop casting) and TiO₂ (dip coating): (a) CNT-WT/TiO₂; (b) CNT-2.5/TiO₂

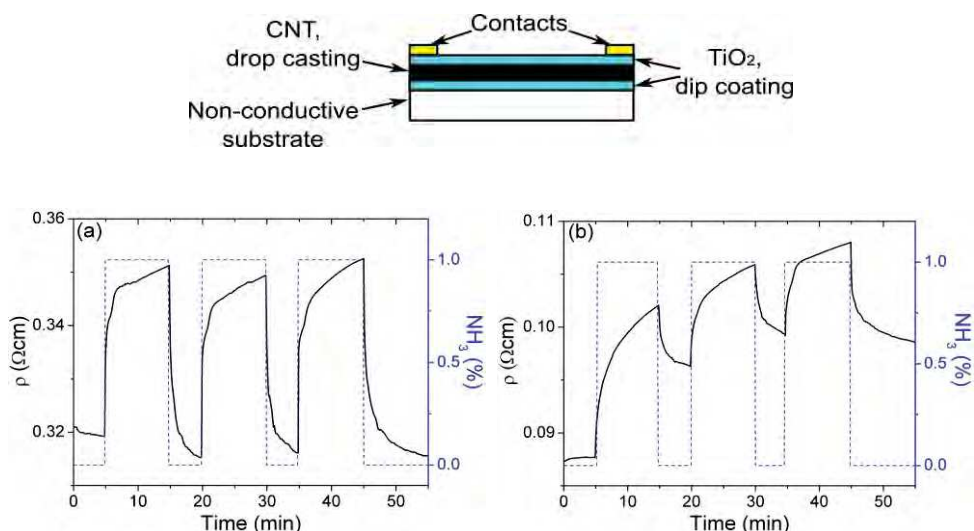


Fig. 10. Dynamical response to ammonia of compound films of CNTs (drop casting) and TiO₂ (dip coating): (a) TiO₂/CNT-WT/TiO₂; (b) TiO₂/CNT-2.5/TiO₂

To quantify the effect of the inclusion of titania layers and the use of functionalized CNTs Figure 11 shows the comparison of the resistivity in air, the sensor response (S_R) (equation 3), the adsorption and desorption times, and the reversibility (equation 4).

$$S_R = R_{\text{ammonia}} / R_{\text{air}} \quad (3)$$

$$R = \Delta R_{\text{desorption}} / \Delta R_{\text{adsorption}} \quad (4)$$

The resistivity in air [Figure 11(a)] shows a decrease up to ~80% when CNTs are covered with titanium dioxide, affecting also the value of S . In titania-free materials, the effect of functionalization is to increase the resistivity in air, while in those containing titania the resistivity decreases and this drop is more notorious in sensors with a higher number of titania layers. With respect to the adsorption/desorption times a clear reduction is observed in the time required for adsorption in functionalized materials, whereas the effect of titania layers is difficult to appreciate. For desorption times, the presence of TiO₂ layers causes up to one order decrease (~90%) and it is far more important than CNT functionalization. The faster sensors correspond to a combination of functionalized CNTs and the presence of TiO₂ layers, see systems CNT-2.5/TiO₂ and TiO₂/CNT-2.5/TiO₂.

Some observations from AFM studies can help to explain the electrical behavior of these composites. Dip coating is a technique that applies strong pressures on the surface as films are deposited (Brinker & Hurd, 1994), therefore it results in the deposition of compact and continuous titania films as was observed by AFM and aids to the formation of new paths for charge carriers. These processes are enhanced if functionalized CNTs are used, giving composites with lower resistivity. There are also some studies that report a larger work function for the TiO₂ than for CNT (Ou et al., 2006; Wang et al., 2005), opening the possibility for electronic transfer from CNT to TiO₂ (Figure 12), increasing the composite conductivity through the increase of titania conductivity and dedoping of CNTs.

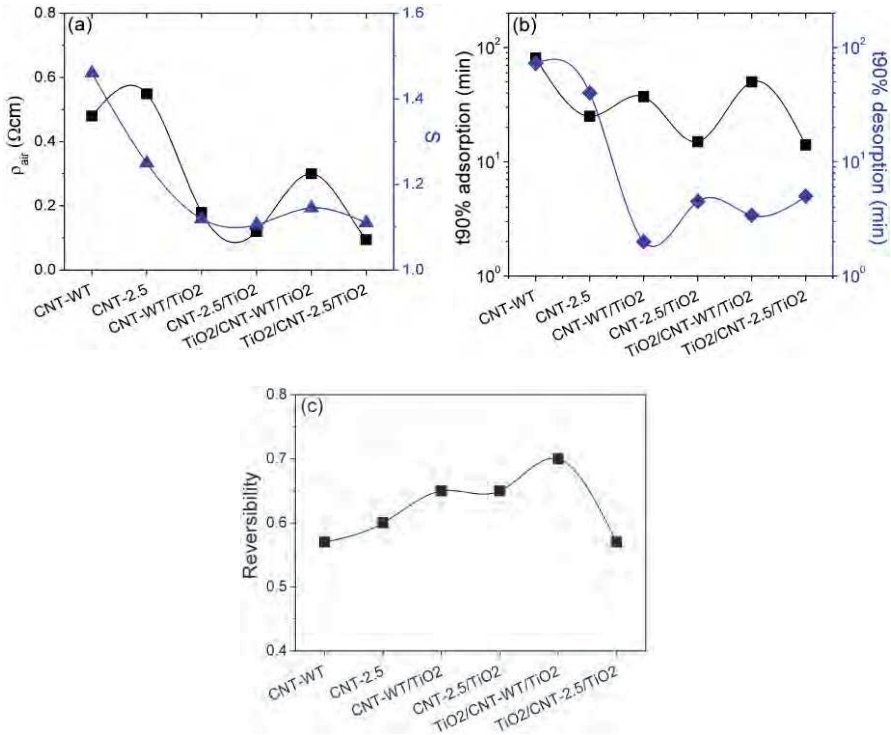


Fig. 11. Characterization of single and multilayer films: (a) resistivity in air and sensor response; (b) adsorption and desorption times; (c) reversibility

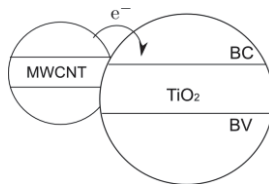


Fig. 12. Electronic transference from MWCNTs to the conduction band of TiO₂

3.3.2 Capacitor sensors

EIS studies of multilayer systems TiO₂/CNT-X/TiO₂ prepared by dip coating and drop casting using CNT-WT and CNT-2.5 are presented in Figures 13 and 14, respectively. Cole-Cole plots are shown in Figures 13(a) and 14(a), the variations of phase angle vs frequency are shown in Figures 13(b) and 14(b), and the results of fitting experimental data with equivalent circuits are presented in Tables 1 and 2. The equivalent circuit used to fit the experimental data of TiO₂/CNT-WT/TiO₂ composite [Figure 13(a)] consists of a resistance R₀ in series with three subcircuits: higher frequencies (R₁C₁), intermediate frequencies (R₂Q₂), and lower frequencies (R₃C₃). The value of R₁ (few ohms) decreases as the material is exposed to ammonia, in contrast to the values of R₂ and of R₃ (several kohms) which show an increase. Capacitance values do

not show a unique tendency either, C_1 increases, C_2 is almost constant, and C_3 decreases with ammonia exposure. Differences among capacitances values are of several orders of magnitude suggesting that adsorption processes are taking place in different sites.

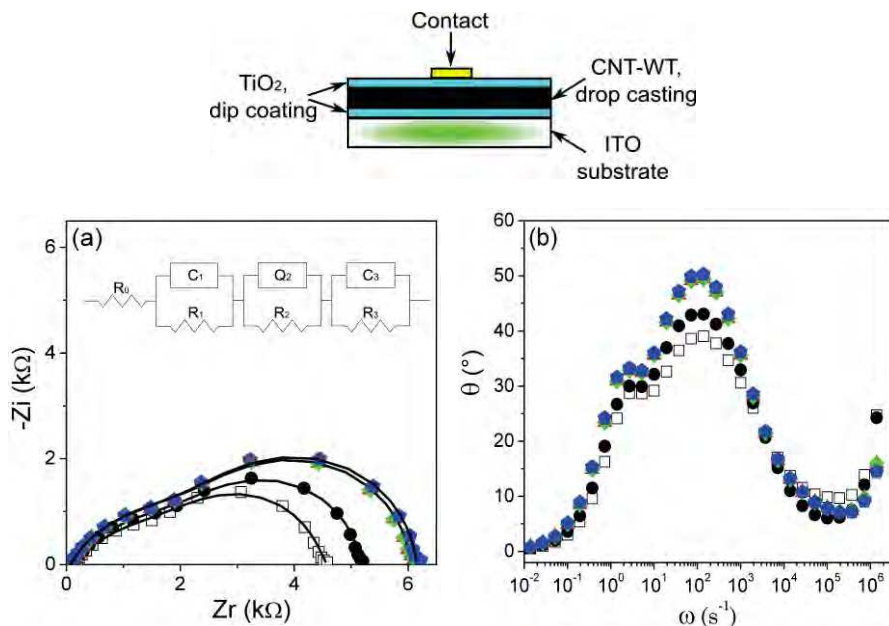


Fig. 13. EIS studies of the composite $\text{TiO}_2/\text{CNT-WT}/\text{TiO}_2$ with CNTs deposited by drop casting and TiO_2 layers prepared by dip coating: (a) Cole-Cole plot; (b) phase angle vs angular frequency. Colors code: white square: air; black circle: NH_3 1 vol.%; red triangle: NH_3 4 vol.%, 5 min; green diamond: NH_3 4 vol.%, 10 min; blue pentagon: NH_3 4 vol.%, 15 min. Markers are experimental data and lines are the fitting results.

In contrast to the multilayer sensor based on non-functionalized CNTs, EIS results of $\text{TiO}_2/\text{CNT-2.5}/\text{TiO}_2$ required only two subcircuits to fit the experimental data depicted in Figure 14. The subcircuit at higher (R_1C_1) and lower (R_2Q_2) frequencies are evident in air, but during ammonia exposure only the process at lower frequencies dominates. R_1 values have been related to TiO_2 grain boundaries in TiO_2 -CNT composites, although the value of $\sim 10^1 \Omega$ is lower than the typical values ($\sim 10^3 \Omega$) (Sánchez et al., 2009), this difference could be related to processes taking place at the CNT/ TiO_2 interface, supporting the improved connectivity of the materials and the direction of charge transfer from CNT \Rightarrow TiO_2 . With respect to the subcircuits at intermediate and lower frequencies in composites based on CNT-WT, changes in capacitances and resistances when the films are exposed to ammonia suggest the presence of two carbon types or two different adsorption sites. In contrast, for composites based on CNT-2.5, amorphous carbon and metal catalysts are removed during functionalization, defining the surface of CNTs as the main adsorption site. Reduction of R_2 in air as well as in ammonia, suggest doping of both TiO_2 and CNTs, because the electronic transference from CNTs to TiO_2 might be facilitated by the formation of covalent bonds during functionalization. Given the tendencies described, we propose that subcircuit 1 is the

Element	Air	1%, 5 min	4%, 5 min	4%, 10 min	4%, 15 min
$R_0(\Omega)$	51	46	46	46	46
$R_1(\Omega)$	53	56	37	26	23
$C_1(\text{nF})$	3.1	2.1	4.3	8.3	11.0
$\tau_1(\mu\text{s})$	0.16	0.11	0.16	0.21	0.25
$\omega_1(\text{s}^{-1}) \times 10^6$	6.08	8.5	6.3	4.6	3.9
$R_2(\text{k}\Omega)$	2.78	2.7	2.9	2.8	2.8
$Q_2^0(\mu\text{Ss}^{\text{n}2})$	35	24	23	22	22
n_2	0.57	0.6	0.7	0.7	0.7
$C_2(\mu\text{F})$	6.0	5.1	5.6	5.9	6.2
$\tau_2(\text{ms})$	17	14	16	17	18
$\omega_2(\text{s}^{-1})$	60	72	62	60	57
$R_3(\text{k}\Omega)$	1.7	2.4	2.9	3.1	3.3
$C_3(\mu\text{F})$	75	65	64	64	62
$\tau_3(\text{s})$	0.12	0.15	0.19	0.20	0.20
$\omega_3(\text{s}^{-1})$	7.8	6.4	5.4	5.0	4.8
S_R		+1.13	+1.30	+1.32	+1.34

Table 1. CNLS fitting results of the system $\text{TiO}_2/\text{CNT-WT}/\text{TiO}_2$, relaxation times and sensor response. The positive value of S_R is to indicate an increase in the resistance

response of titania grain boundaries, subcircuit 2 is the response of CNTs, and subcircuit 3 is related to the response of impurities in CNT-WT, these correlations are summarized in Table 3. The removal of impurities (i.e. elimination of the third subcircuit) and the decrement in R values reduce the relaxation times up to three orders of magnitude, from seconds for composites with CNT-WT to milliseconds for composites with CNT-2.5. Another benefit of the functionalization is that the capacitance response computed from equation 5 increases up to ~ 2.5 (i.e., 150%, Table 2) in composites with CNT-2.5, which is about one order higher than the response of resistors [~ 1.2 , i.e., 20%, Figure 11(a), Tables 1 and 2].

$$S_C = C_{\text{ammonia}} / C_{\text{air}} \quad (5)$$

Element	Air	1%, 5 min	4%, 5 min	4%, 10 min	4%, 15 min
$R_0(\Omega)$	26				
$R_1(\Omega)$	31				
$C_1(\text{nF})$	44				
$\tau_1(\mu\text{s})$	1.3				
$\omega_1(\text{s}^{-1}) \times 10^5$	7.3				
$R_2(\Omega)$	168	219	220	222	222
$Q_2^0(\mu\text{Ss}^{\text{n}2})$	55	19	15	14	14
n_2	0.6	0.7	0.8	0.8	0.8
$C_2(\mu\text{F})$	1.4	2.5	2.9	3.2	3.4
$\tau_2(\text{ms})$	0.23	0.54	0.64	0.69	0.76
$\omega_2(\text{s}^{-1}) \times 10^3$	4.2	1.8	1.5	1.4	1.3
S_R		+1.106	+1.097	+1.104	+1.112

Table 2. CNLS fitting results of the system $\text{TiO}_2/\text{CNT-2.5}/\text{TiO}_2$, relaxation times and sensor response. The positive value of S_R is to indicate an increase in the resistance

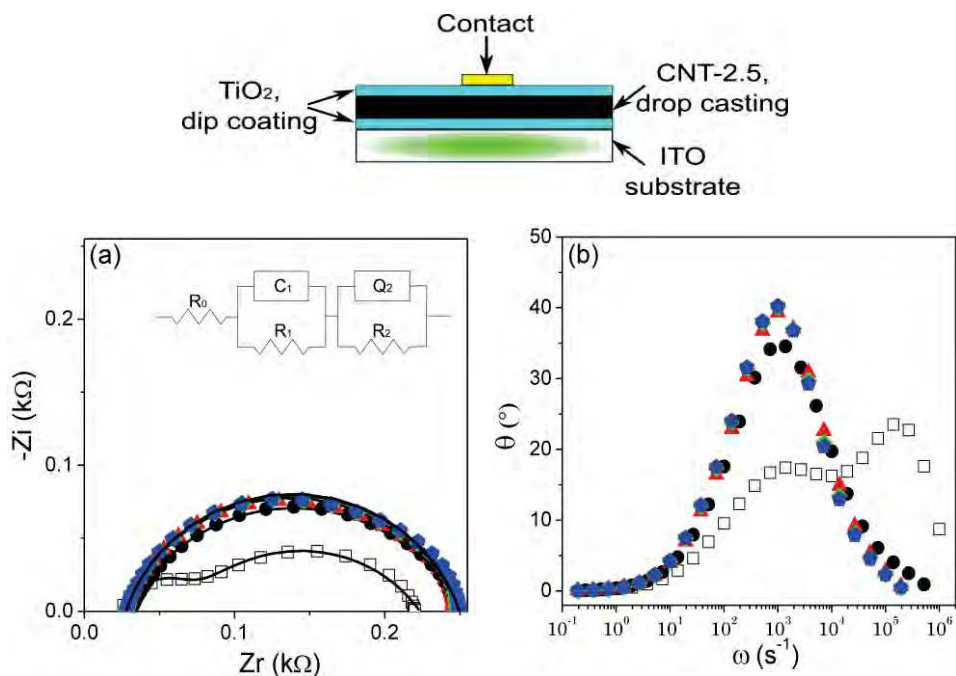


Fig. 14. EIS studies of $\text{TiO}_2/\text{CNT-2.5}/\text{TiO}_2$ composite with CNTs deposited by drop casting and TiO_2 layers prepared by dip coating: (a) Cole-Cole plot; (b) phase angle vs. angular frequency. Colors code: white square: air; black circle: NH_3 1 vol.%; red triangle: NH_3 4 vol.%, 5 min; green diamond: NH_3 4 vol.%, 10 min; blue pentagon: NH_3 4 vol.%, 15 min. Markers are experimental data and lines are fitting results.

CMP-WT	CMP-2.5	Correlation
R_0	R_0	Resistance due to external connectors
R_1C_1	R_1C_1 (only in air)	TiO_2 grain boundaries
R_2Q_2	R_2Q_2	Carbon nanotubes
R_3C_3		Amorphous carbon and impurities

Table 3. Correlation of the equivalent circuits elements with the adsorption sites of the multilayered composites CMP-WT and CMP-2.5

4. Conclusions and future directions

Design of composite materials based on combinations of nanoparticled titanium dioxide and multiwalled carbon nanotubes, using small amounts of nanotubes for low cost room temperature ammonia sensors have been demonstrated. For sensor fabrication, *ex situ* synthesis of TiO_2 and functionalization of CNTs were carried out separately and deposited

in a multilayer configuration. Composites were tested as resistors and capacitors during ammonia sensing based on CNTs functionalization and number of titania layers. Results indicated that the use of titania layers in combination with the substantial chemical oxidation of CNT surface produced a better material with synergistic properties for sensing applications.

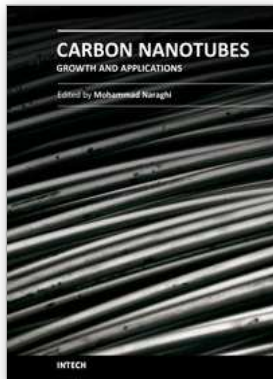
5. Acknowledgment

We acknowledge the fellowship provided by the Consejo Nacional de Ciencia y Tecnología, CONACYT-México (M. Sánchez), we thank to M.L. Ramón García for the XRD analysis and to P. Altuzar Coello for TGA analysis.

6. References

- Adu, C.K.W.; Sumanesekera, G.U.; Pradhan, B.K.; Romero, H.E. & Eklund, P.C. (2001), Carbon nanotubes: a thermoelectric nano-nose, *Chemical Physics Letters*, Vol. 337, pp. 31-35.
- An, G.; Ma, W.; Sun, Z.; Liu, Z.; Han, B.; Miao, S.; Miao, Z. & Ding, K. (2007), Preparation of titania/carbon nanotube composites using supercritical ethanol and their photocatalytic activity for phenol degradation under visible light irradiation, *Carbon*, Vol. 45, pp. 1795-1801.
- Brinker, C.J. & Hurd, A.J. (1994), Fundamentals of sol-gel dip coating, *Journal de Physique III*, Vol. 4, pp. 1231-1242.
- Cullity, B.D. (1978). *Elements of X-Ray Diffraction*, Addison-Wesley, Massachusetts, USA.
- Espinoza, E.H.; Ionescu, R.; Chambon, B.; Bedis, G.; Sotter, E.; Bittencourt, C.; Felten, A.; Pireaux, J.J.; Correig, X. & Llobet, E. (2007), Hybrid metal oxide and multiwall carbon nanotube films for low temperature gas sensing, *Sensors and Actuators B: Chemical*, Vol. 127, pp. 137-142.
- Hieu, N.V.; Duy N.V.; Huy, P.T.; Chien, N.D.; Thamilselvan, M. & Yi, J. (2008), Mixed SnO₂/TiO₂ included with carbon nanotubes for gas-sensing application, *Physica E*, Vol. 41, pp. 258-263.
- Jhi, S.H.; Louie, S.G. & Cohen M.L. (2000), Electronic properties of oxidized carbon nanotubes, *Physical Review Letters*, Vol. 85, pp. 1710-1713.
- Ong, K.G.; Zeng, K. & Grimes C.A. (2002), A wireless, passive carbon nanotube-based gas sensor, *IEEE Sensors Journal*, Vol. 2, pp. 82-88.
- Ou, Y.; Lin, J.; Fang, S. & Liao, D. (2006), MWNT-TiO₂: Ni composite catalyst: A new class of catalyst for photocatalytic H₂ evolution from water under visible light illumination, *Chemical Physics Letters*, Vol. 429, pp. 199-203.
- Peng, S. & Cho, K. (2003), Ab initio studies of doped carbon nanotube sensors, *Nano Letters*, Vol. 11, pp. 57-60.
- Sánchez, M. & Rincón M.E. (2009), Sensor response of sol-gel multiwalled carbon nanotubes-TiO₂ composites deposited by screen-printing and dip-coating techniques, *Sensors and Actuators B: Chemical*, Vol. 140, pp. 17-23.
- Sánchez, M.; Rincón M.E. & Guirado-López R.A. (2009), Anomalous sensor response of TiO₂ films: electrochemical impedance spectroscopy and ab initio studies, *The Journal of Physical Chemistry C*, Vol. 113, pp. 21635-21641.

- Song, H.; Qiu, X.; Li, F.; Zhu, W. & Chen, L. (2007), Ethanol electro-oxidation on catalysts with TiO₂ coated carbon nanotubes as support, *Electrochemistry Communications*, Vol. 9, pp. 1416-1421.
- Stan, G. & Cole, M.W. (1998), Hydrogen adsorption in nanotubes, *Journal of Low Temperature Physics*, Vol. 110, pp. 539-544.
- Valentini, L.; Cantalini, C.; Armentano, I.; Kenny, J.M.; Lozzi, L. & Santucci, S. (2004), Highly sensitive and selective sensors based on nanotubes thin films for molecular detection, *Diamond and Related Materials*, Vol. 13, pp. 1301-1305.
- Varghese, O.K.; Kichambre, P.D.; Gong, D., Ong, K.G.; Dickey, E.C. & Grimes, C.A. (2001), Gas sensing characteristics of multi-wall carbon nanotubes, *Sensors and Actuators B: Chemical*, Vol. 81, pp. 32-41.
- Villalpando-Páez, F.; Romero, A.H.; Muñoz-Sandoval, E.; Martínez, L.M.; Terrones, H. & Terrones, M. (2004), Fabrication of vapor and gas sensors using films of aligned CN_x nanotubes, *Chemical Physics Letters*, Vol. 386, pp. 137-143.
- Wang, W.; Serp, P.; Kalck, P. & Faria, J.L. (2005), Photocatalytic degradation of phenol on MWNT and titania composite catalysts prepared by a modified sol-gel method, *Applied Catalysis B*, Vol. 56, pp. 305-312.
- Williams, K.A. & Eklund, P.C. (2000), Monte Carlo simulations of H₂ physisorption in finite-diameter carbon nanotube ropes, *Chemical Physics Letters*, Vol. 320, pp. 352-358.
- Yu, H.; Quan X.; Chen, S. & Zhao, H. (2007), TiO₂-multiwalled carbon nanotube heterojunction arrays and their charge separation capability, *The Journal of Physical Chemistry C*, Vol. 111, pp. 12987-12991.
- Zhao, J.; Buldum, A.; Han, J. & Lu, J.P. (2002), Gas molecule adsorption in carbon nanotubes and nanotube bundles, *Nanotechnology*, Vol. 13, pp. 195-200.



Carbon Nanotubes - Growth and Applications

Edited by Dr. Mohammad Naraghi

ISBN 978-953-307-566-2

Hard cover, 604 pages

Publisher InTech

Published online 09, August, 2011

Published in print edition August, 2011

Carbon Nanotubes are among the strongest, toughest, and most stiff materials found on earth. Moreover, they have remarkable electrical and thermal properties, which make them suitable for many applications including nanocomposites, electronics, and chemical detection devices. This book is the effort of many scientists and researchers all over the world to bring an anthology of recent developments in the field of nanotechnology and more specifically CNTs. In this book you will find:

- Recent developments in the growth of CNTs
- Methods to modify the surfaces of CNTs and decorate their surfaces for specific applications
- Applications of CNTs in biocomposites such as in orthopedic bone cement
- Application of CNTs as chemical sensors
- CNTs for fuelcells
- Health related issues when using CNTs

How to reference

In order to correctly reference this scholarly work, feel free to copy and paste the following:

Marciano Sánchez and Marina Rincón (2011). Ammonia Sensors Based on Composites of Carbon Nanotubes and Titanium Dioxide, Carbon Nanotubes - Growth and Applications, Dr. Mohammad Naraghi (Ed.), ISBN: 978-953-307-566-2, InTech, Available from: <http://www.intechopen.com/books/carbon-nanotubes-growth-and-applications/ammonia-sensors-based-on-composites-of-carbon-nanotubes-and-titanium-dioxide>

INTECH
open science | open minds

InTech Europe

University Campus STeP Ri
Slavka Krautzeka 83/A
51000 Rijeka, Croatia
Phone: +385 (51) 770 447
Fax: +385 (51) 686 166
www.intechopen.com

InTech China

Unit 405, Office Block, Hotel Equatorial Shanghai
No.65, Yan An Road (West), Shanghai, 200040, China
中国上海市延安西路65号上海国际贵都大饭店办公楼405单元
Phone: +86-21-62489820
Fax: +86-21-62489821

© 2011 The Author(s). Licensee IntechOpen. This chapter is distributed under the terms of the [Creative Commons Attribution-NonCommercial-ShareAlike-3.0 License](#), which permits use, distribution and reproduction for non-commercial purposes, provided the original is properly cited and derivative works building on this content are distributed under the same license.